Trends in Analytical Chemistry 89 (2017) 190–196

Contents lists available at ScienceDirect

Trends in Analytical Chemistry

journal homepage: www.elsevier.com/locate/trac

Fourier-transform *vs.* quantum-cascade-laser infrared microscopes for histo-pathology: From lab to hospital?

Abiodun Ogunleke [a], Vladimir Bobroff [a], Hsiang-Hsin Chen [b], Jeremy Rowlette [c], Maylis Delugin [a], Benoit Recur [a], Yeukuang Hwu [b], Cyril Petibois [a, b, *]

[a] University of Bordeaux – Inserm U1029 LAMC, Allée Geoffroy Saint-Hillaire, Bat B2, 33600, Pessac, France
[b] Academia Sinica, Institute of Physics, Nankang, Taipei, 115, Taiwan
[c] Daylight Solutions, 15378 Avenue of Science #200, San Diego, CA, 92128, United States

ARTICLE INFO

Article history:
Available online 27 February 2017

Keywords:
FTIR microscopy
QCL-IR imaging
3D chemical imaging
Digital pathology
Clinical routine

ABSTRACT

IR microscopy was first conceptualized in 1949 and the first commercial system was launched 1983. With the appearance of FPA detectors in the 90's, FTIR microscopy became a technique of choice for histology. Two decades later, the release of QCLs working in the mid-IR range refuels this promise by accelerating tremendously the acquisition of IR images for large tissue areas with high-quality spectra for chemical mapping of parameters of interest.

The new QCL-IR imaging system allows a 150× faster spectral data acquisition at equivalent S/N level. The quality of spectral data is comparable while applying spectral curve-fitting treatments, thus showing that laser sources offer reliable signal over a large spectral range. If QCL-IR imaging system seem to offer the opportunity to develop routines for anatomo-pathology, several technological challenges stand in front of us to reach this goal to define the specs of an IR microscope dedicated to hospital.

1. Introduction

Pathologists have experienced and adopted many changes in the laboratory, including the use of cryomicrotomes and slide cassettes, tissue embedding systems, and the development of immuno-histochemistry (IHC) starting in the 80s. However, anatomo-pathology is still mostly manual. There exist high-throughput slide scanners and IHC can be automated, but this is for repetitive tasks only (analyzing long series of tissue section in the same way or accumulating databases). For anatomo-pathology, interpretation of data requires a proper lecture at the details found in the tissue. The main bottleneck here remains the slow computerization and the lack of automation for the “lecture” part of the pathologist's activity. If computer-assisted analysis and storage of tissue images now includes automated slide labeling and referencing, it has also possibly restricted the range of analyses that pathologists are seeking in routine cases: for example, electron microscopy analyses are available but remain too complex for routine, thus forcing pathologists to move back to a limited number of IHC antibodies and molecular pathology tests. These IHC antibodies can be read immediately and their distribution is the meaningful information that is sought. This is synonymous of very slow progress where the demand for high-performance in analytics is raising exponentially, notably to obtain more and more information from tissue contents.

Laboratories benefit from automated labeling systems for high-throughput analyses, thus able to sustain an increasing demand of diagnostic parameters from different clinical services. However, labeling methods and instruments have intrinsic limits that are unlikely to be circumvented in the future. The lack of quantitative information and the dependence on the pathologist's expertise for the interpretation of results are other issues. Furthermore, biopsies are not benefiting from imaging technologies, the *in vivo* condition requiring the use of contrast agents that diffuse efficiently only in living systems [1]. From an *ex vivo* specimen of a tissue, the molecular parameters can be analyzed by the application of mass-spectrometry (MS) imaging and hydrogel devices for histology applying tissue protein digestion [2]. For electron microscopy also, sections thinner than 100 μm can be analyzed in detail. However, these techniques require heavy workload compared to the routine anatomo-pathology activities. Actually, they even failed to be properly introduced in the clinics' pathology services a decade ago,

* Corresponding author. University of Bordeaux – Inserm U1029 LAMC, Allée Geoffroy Saint-Hillaire, Bat B2, 33600, Pessac, France.
E-mail address: petibois@gate.sinica.edu.tw (C. Petibois).

http://dx.doi.org/10.1016/j.trac.2017.02.007
0165-9936/

being abandoned by pathologists because of their complexity, synonymous of low reliability.

Alternatively, the chemical analysis of tissues can be also performed by reagent-free microscopies, such as those derived from vibrational spectroscopy (infrared and Raman) [3]. Combining a spectrometer and a microscope is called spectro-microscopy. These setups offer a global view of the sample chemical contents, which can be treated for extracting relevant molecular parameters for diagnosis. They can thus perform a 2D chemical mapping with a lateral resolution of a few microns only, which reaches the cellular scale in tissues. They are also reagent-free and do not require fixing the tissue before data acquisitions, thus ensuring to analyze the native tissue with all its components maintained like in the *in vivo* condition. Besides these presumed advantages, they have not been considered so far for routine histology in clinics, which is due to their slow process in image acquisition for large tissue areas [4]. In analytical chemistry, the other challenge of spectro-microscopy is to overcome the complexity and big size of spectral data found in large images [5] if new analytical tools must be provided for routine histology.

1.1. Spectroscopy in histology

Why should spectro-microscopy be a relevant technique for routine histopathology? Cutting-edge techniques in molecular and cell-based diagnostics are already used in hospitals, such as flow cytometry, DNA screening and gene sequencing, fluorescence *in situ* hybridization, and proteomics. These changes undertaken by the analytical materials of anatomo-pathology collectively represent a clear direction for technological innovation in the field. However, they also bring possible threats and dead ends. For example, digital pathology is by far more complex than just making the acquisition of a digital image of the tissue section. It includes a sequence of computer-assisted events that must handle the acquisition, storage, treatment, analysis, visualization, and interpretation of tissue contents. In this technical chain, the first step, acquisition of images, already suffers from major problems of reliability, a prerequisite for automation. For example, if we use a UV-confocal microscope to highlight the distribution of label, this one will be revealed by adjusting the laser source power depending on the quality of the antibody–ligand interaction. This is making UV-confocal microscopy a semi-quantitative or simply qualitative imaging techniques. This slack of quantitative signal management compromises the automation of data treatments.

To become a routine, digital pathology will require an automation of these events at several levels: 1 – automating the extraction of parameters of interest from digital images; 2 – automating the comparison between reference (or healthy, pathological) and new tissue slides; 3 – automating the diagnostic information to extract; 4 – allowing the system to work in a non-supervised fashion, thus making feasible the recognition of abnormal features in a tissue. This last feature must be validated by the physician, but 90% of the work must be automated without risk of interpretation errors, thus in a supervised way. The supervised features will be considered as standard diagnostic tools while the non-supervised ones might be considered as exploratory parameters. Supervised here means that the pathologists decided in advance which tissue feature he wants to reveal, most of time by using a dedicated label, there is thus no other information to expect. Unsupervised means that there is no *a priori* decision taken to reveal a given feature. Optical visible microscopy is a good example of unsupervised analysis of a tissue sample, but it is restricted to the interaction of light with density changes in the tissue, which thus mainly highlight its anatomical organization.

For more sophisticated unsupervised analyses of tissue contents, chemical imaging techniques (infrared, mass, Raman and others) can play a unique role because of the global nature of the chemical information they provide. For the past two decades, Fourier-transform infrared (FTIR) microscopy has been used for developing histological methods [6], mostly in cancer research [7–10]. Other applications include the analysis of bone osteoporosis [11] and osteoarthritis [12], myopathies [13], dermopathies [14], liver fibrosis [15], degenerative diseases [16], etc. It is useful for histology thanks to the global chemical information it provides about the sample [17]. Global means that all chemical bonds present in the sample will raise absorption bands, notably for proteins and lipids, which exhibit intense absorptions [18], but also with major contribution from carbohydrates [19] and nucleic acids [20] to the final spectral information. Because it is quantitative, it also allows mapping potentially a wide range of chemical information in a non-supervised pattern, which is undoubtedly a major advantage for comparison between healthy and pathological tissue specimens without any *a priori* knowledge about the sample A search for publications on pubmed (as of Dec. 31st, 2016 – Supplementary material, Fig. S1), shows that FTIR microscopy has been associated to about 6000 histological studies, amongst which cancer and bone pathology have been the main issues.

1.2. IR microscopy in histology

FTIR microscopy is particularly well suited for tumor imaging as it provides high contrast between healthy and tumor tissues, these ones being usually characterized by major redistributions between proteins and lipids contents [21]. For bone, this is due to the very characteristic absorptions found from carbonate ions of hard tissues [22] in a spectral region not covered by proteins (main spectral region 1700–1480 cm^{-1}) and lipids (main spectra region 3050–2800 cm^{-1}), i.e. the 1300–1100 cm^{-1} spectra region [11]. These two most important topics of IR microscopy in histological studies are followed by skin analysis. This is due to the accessibility of the sample (surface of the body), so that attenuated-total-reflectance devices can be used for '*in vivo*" measurements. 374 manuscripts among the 931 references in pubmed are related to the use of attenuated total reflectance (ATR) FTIR devices for direct measurements on skin. This is also due to the fact that the skin surface has a well characterized lipid composition that can be accurately analyzed by FTIR spectroscopy [23,24].

Other pathological organs are less studied by spectroscopists, possibly due to the anatomical complexity of the samples, which limits the interpretation of data obtained from small tissue areas, usually <1 mm^2. This is particularly true for brain, kidney, pancreas and liver, which exhibit complex sub-structure organizations and networks (like neurons, blood vessels, multiple cell phenotypes… etc.). This is thus challenging the FTIR microscopy community with the request of new methods allowing to capture large IR images of tissue, i.e. at the dimension of clinical biopsies frequently in the range of the 1 cm^2. At diffraction limited resolution, i.e., about 5–10 μm for the mid-IR range, the acquisition of 1 cm^{-1} tissue area will be too long (hours) at sufficient spectral quality (S/N ≥ 100) for routine cases.

Since 2013, there has been a marked decline in the number of publications related to FTIR-based histology, possibly a sign of reluctance due to the lack of significant analytical performance improvement since the appearance of FPA detectors 15 years ago. In the meantime, outstanding developments occurred for other histological techniques, promising "high-resolution", "time-resolved", "*in vivo*", and "3D" capability. None of these analytical performances have been achieved by IR microscopy, with the exception of some home-made optical setups which have not yet been

marketed. Their weakness is the lack of reliability in providing the same result fast enough and without using inaccessible means. For example, the use of synchrotron radiation to enhance the S/N level has been justified by the pursuit of getting better analytical performances out of catalog FTIR microscopes [25,26]. However, this is remaining at the demonstration level since synchrotron radiation centers cannot be used for a routine business.

It means that innovation in FTIR microscopy technology is required to refuel the interest on this technique for histology. This is actually occurring with the use of intense IR sources, namely quantum cascade lasers (QCL) working collectively to cover a large part of the mid-IR range, currently the 1800–830 cm^{-1} interval [27]. The release of QCL-IR microscopes has the potential for reinventing our approach of histology by speeding up the acquisition process at high S/N. But what the speed is going to bring for the new utilizations of this "Fourier-transform-free" IR microscopy remains to be determined.

2. Comparison between FTIR and QCL-IR microscopy for histological analysis

FTIR microscopes are setup with arrays of detectors, in linear or focal plane array (FPA) geometry, these ones bearing up to 128 × 128 individual detectors (Fig. 1). During the acquisition, the FPA detector receives all wavelengths thanks to an interferometer (Michelson). An interferogram is generated and a Fourier transform is used to convert it into an actual spectrum. FTIR microscope equipped with a FPA use a thermal Globar source of IR photons that the interferometer can manage to provide all desired wavelength in a spectral region (4000–500 cm^{-1} for the mid-infrared region).

QCLs are semiconductor lasers that emit in the mid-to far-infrared portion of the electromagnetic spectrum. In quantum cascade structures, electrons undergo intersubband transitions and photons are emitted. The electrons tunnel to the next period of the structure and the process repeats. Therefore, unlike IR interferometers, QCLs generate the mid-IR signal wavelength-by-wavelength in absolute values and the spectrum reconstruction does not require the Fourier transform anymore [28]. Because of this wavelength-by-wavelength signals generation, obtaining a large spectral region may take time, but the development of pulsed lasers working in the ms range has probably compensated the periodic mode of signal generation [29]. This is also due to the fact that QCLs are currently covering a quite limited spectral interval, usually no more than 100–300 cm^{-1}. The combination and modulation of several QCLs is thus required to cover a large spectral region, as for FTIR setups.

The first ever released microscope powered by QCL-IR sources, Spero® came from Daylight Solutions (San Diego, California) in 2014. Compared to current FTIR microscopes offering equivalent imaging capabilities, i.e. equipped with a large focal-plane array (FPA) detector and motorized sample stage for acquisition of large sample areas, this QCL-IR microscope promises much higher S/N than FTIR systems thanks to the high-power output (photon flux) of lasers, but it is limited to a shorter spectral interval (1800–830 cm^{-1} – see Table 1 for specifications). We conducted a series of measurements to test the system in its full specifications, i.e., by collecting all wavelengths for a spectral analysis of tissue sample contents. In brief, both the FTIR and the QCL-IR systems were used for analyzing the same tissue sections of a mouse brain (total area has a diameter of ~9 mm) in which a glioma tumor was grown.

The S/N of an FTIR spectrometer is used to measure its sensitivity and is often considered as the primary specification for determining whether an instrument will meet the needs of intended use (Fig. 2). The S/N was roughly 50% higher with a single scan using the QCL-IR system than with the best acquisition condition (1000 scans) for the FTIR system. The comparison is even more striking if we consider that the tissue area covered by a single FPA tile dimension acquisition, is 340 × 340 μm^2 for the FTIR system (2.66 × 2.66 μm^2/pixel) and 2000 × 2000 μm^2 for the QCL-IR system (4.3 × 4.3 μm^2/pixel). One may also mention the speed of acquisition in terms of pixels/second, which is ranging from 2044 (S/N of 20 ± 8) to 1 (S/N of 490 ± 100) for the FTIR system. A reasonable comparison would be the 743 pixels/sec for FTIR using 10 scans (S/N of 63 ± 21) with the 768 pixels/sec for QCL-IR using 1 scan (S/N of 841 ± 210). At equivalent rate of spectra acquisition (or pixels), the QCL-IR system provides a 13 times higher S/N than the FTIR microscope. It has been hypothesized that QCL-IR systems could perform acquisitions 1000× faster than FTIR at comparable SNR and resolutions (spectral and lateral) [30]. Here, if we consider the area covered and the final pixel size obtained and the speed of acquisition, we obtained an IR image of a large tissue area (a mouse brain tissue section of a Ø ~7 mm; see Fig. 3) ~150 faster with the QCL-IR system.

Taken together, this gap in S/N level and the higher speed of acquisition are critical features for developing new applications of IR microscopy, notably the analysis of large tissue samples [31]. In Fig. 3, we show the analysis of the mouse brain tissue section. The

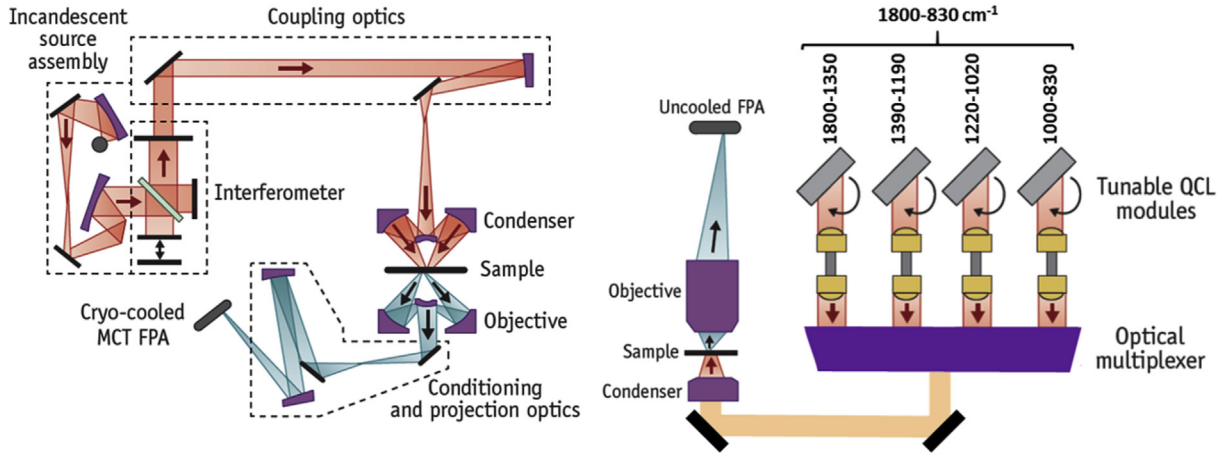

Fig. 1. Schematic setup of FTIR and QCL based IR microscopes. Images courtesy from DaylightSolutions®.

Table 1
Basic specifications of compared IR microscopy systems.

Type	Resolution (cm^{-1})	Spectral range (cm^{-1})	Detector size (μm)	FPA type (pixels, condition)	FPA coverage (mm)	Mag. levels	Final pixel size (μm)	FOV (μm)
FTIR	1–16…	4000–400	40 × 40	128 × 128	5.12 × 5.12	15X	2.66 × 2.66	340 × 340
				N_2-cooled		36X	1.1 × 1.1	140 × 140
QCL-IR	4 and 8	1800–830	17 × 17	480 × 480	8.16 × 8.16	4X	4.25 × 4.25	2000 × 2000
				Uncooled		12.5X	1.36 × 1.36	650 × 650

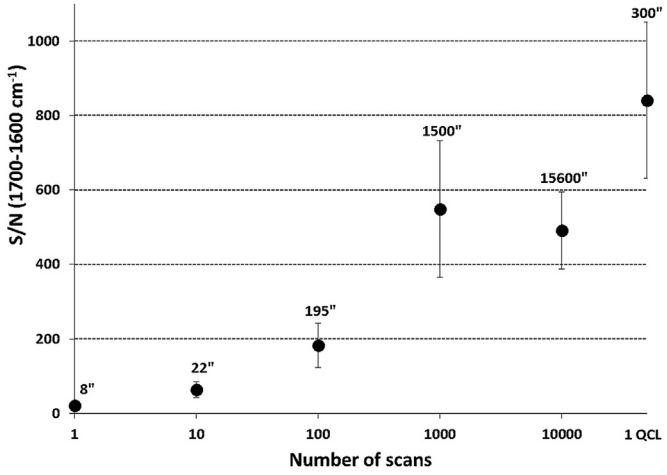

Fig. 2. S/N measured on FTIR and QCL-IR microscopes using the 1800–1700 cm^{-1} spectral interval. Acquisition time is given in the data panel of the figure and expressed in seconds. The S/N values are mean from a full FPA tile (128 × 128 elements for N_2-cooled FTIR system and 480 × 480 elements for uncooled QCL-IR system).

FTIR system with a 128 × 128 FPA detector required patching 25 × 22 IR images, for a total acquisition time of 11–12 h using 25 scans at 8 cm^{-1} and with an 8 × 8 binning (thus obtaining a 20-μm pixel resolution on final image), which is the best compromise to maintain the cross-reference between background and sample acquisitions (total acquisition of 9 million spectra, 141,000 spectra after the 8 × 8 binning). The FTIR system was constantly purged with filtered dry-air in an air-conditioned room (20°C, 65% humidity). The sample stage of the microscope was protected by a plastic box to optimize the purge, and the FPA detector was refiled with liquid N_2 in top-up mode (every 30 min to maintain full N_2 volume and thus avoid any temperature fluctuation at detector location) by automated pump (Norhof LN_2 Microdosing System #905, Germany). These analytical conditions can be considered as optimized for IR microscopy, avoiding ambient condition changes over the complete acquisition period.

The QCL-IR microscope was used at 4.3 × 4.3 $μm^2$ pixel resolution with a single scan at 8 cm^{-1} and required 5 × 4 FPA tiles (480 × 480 pixels each) obtained in 109 min (S/N 870 ± 190). A total of 4.6 million spectra was obtained for the mouse brain tissue section. It allows obtaining similar chemical mapping using the same spectral intervals than with the FTIR system. The lipid-to-protein ratio calculated from the 1430–1480 and 1700–1480 cm^{-1} spectral intervals exhibited comparable intensity ranges. The protein to lipid ratio was also processed and reconstructed IR images were found similar in intensity range and distribution within the tissue section, the anatomical details of brain tissue appearing clearly. Therefore, at a macroscopic level (ca. a 1-cm^2 tissue section area), the two systems provide very similar results. To compare the results at the spectrum level (Fig. 4), we further compared the absorption parameters for a series of twenty pixels of 4.3 × 4.3 × 10 $μm^3$ for the QCL system and 5.2 × 5.2 × 10 $μm^3$ for the FTIR system (using a 2 × 2 binning of spectra for closest matching of voxel dimensions – spectra extracted from same tissue region, see Fig. 4). We used the curve-fitting method as an example of spectral data treatment that highlights spectral absorption differences. The curve-fitting of the 1750–1450 cm^{-1} spectral interval (amide I and II of proteins) is a widely-used method for characterizing the secondary structure of proteins. It allows extracting several bands for which the protein structure parameter can be assigned. We applied a fixed band profile (position of bands in the amide I spectral interval) and let the mathematical parameters of band shape (full-width at half

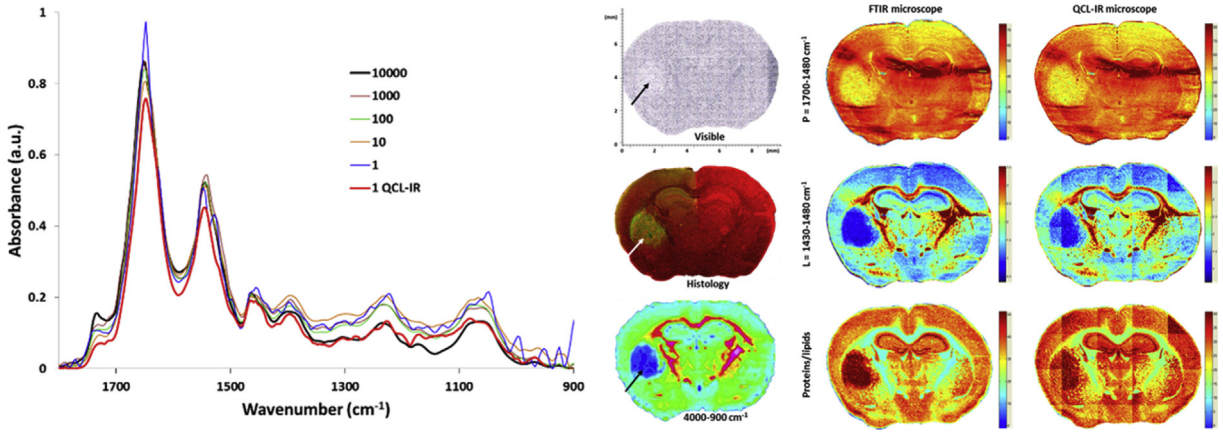

Fig. 3. Comparison of IR spectra and 2D mapping of major absorptions on large tissue area. IR spectra corresponding to the same tissue location for the different scanning time shown in Fig. 3 are presented in left panel. Right panel shows IR images: Left: IR spectra extracted from IR images at different acquisition conditions on both the FTIR and QCL-IR microscopes. Left: The tumor implantation is shown with black arrow on visible (top) image and corresponding labeling of tumor cells (vimentin – green) is observed on histological (immunofluorescence – center) image (white arrow indicate tumor location). The full spectral absorbance IR image (bottom) from FTIR microscope is obtained in a 12 h-acquisition. Middle: FTIR images are shown for proteins (top: P = 1700–1480 cm^{-1}) and lipids (center: L2 = 1480–1430 cm^{-1}) absorbance. The protein to lipid ratio is calculated and image reconstructed (bottom). Comparative results are presented for QCL-IR microscope (right column).

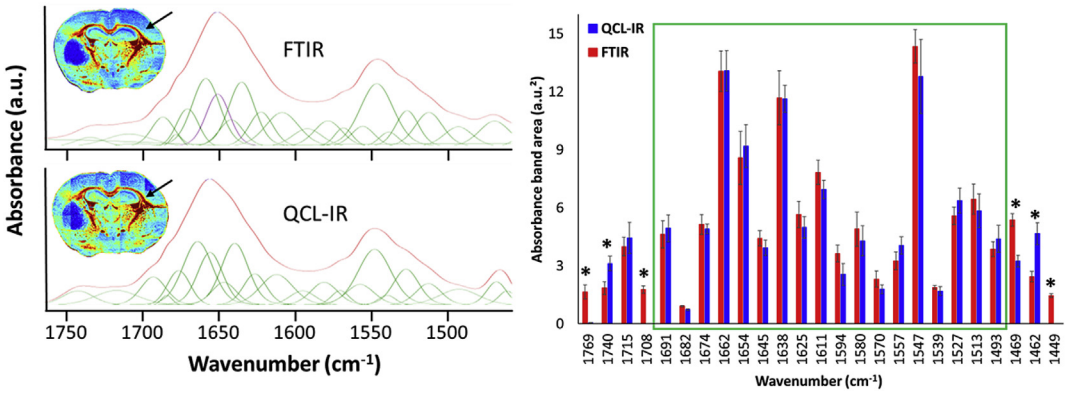

Fig. 4. Curve-fitting of the 1750–1600 cm^{-1} spectral interval using common band distribution profile. Twenty spectra were extracted on the same area of the cortex as indicated by arrows, choosing a common location on FTIR and QCL-IR images. Curve-fitting was processed after baseline correction (1800–900 cm^{-1}). Band parameters were set as follows: 20/80 Gaussian/Lorentzian, band positions peaked from second derivative spectra and fixed for the 1700–1490 cm^{-1} spectral interval and let free for extremities (i.e., >1700 cm^{-1} and <1490 cm^{-1}). A 0.1 RMSE error was set as a limit for curve-fitting calculation. * = $p < 0.05$.

height, Gaussian/Lorentzian fraction, intensity at band position) free in the curve-fitting process [5].

The curve-fitting of spectra obtained by the FTIR and QCL IR microscopes at closest S/N (1000 scans for FTIR *vs.* single scan for QCL) shows that band distribution and shape for the amide I and II area (shown as the green rectangle on Fig. 4) are rather similar with a low RMESE value obtained for each spectrum reconstruction (<0.1% of spectral interval area). However, bands found at the limit of QCL-IR spectral range coverage (i.e., approaching 1800 cm^{-1}) had significant variations with respect to the FTIR spectra. This is possibly due to the cutoff of signal for the laser covering this spectral region. Other variations were also observed at the right limit of the spectral interval used for the curve-fitting (i.e., approaching 1450 cm^{-1}). The shape of the QCL-IR and FTIR spectra were quite different below 1500 cm^{-1}, thus inducing those significant deviations in related curve-fitted bands. This is certainly due to a difference in signal distribution over the spectral interval covered by the respective sources for the FTIR and QCL-IR microscopes. The shift from one laser to another in the QCL-IR systems (powered by 4 lasers for the 1800–950 cm^{-1}) can induce a loss of linearity in signal that must be taken into account. Thus, even if curve-fitted parameters were found very close between techniques for the amide I and II region, the comparison between microscopes powered by different IR sources must be considered very cautiously. Such differences between IR spectra obtained by different systems is not surprising as it was already observed between FTIR systems powered by the globar and synchrotron radiation sources [26,32].

3. Discussion

3.1. The source-detector issue revisited

Till now, the source-detector issue was the bottleneck of infrared microscopy [17]. A weak photon flux was observed while using Globar sources and that FPA detectors remained poorly sensitive due to the lack of challenging performances of Globar-based optical systems. With the arrival of more powerful laser sources, the use of detectors with more linear response (microbolometer FPAs) seems feasible and thus to bring a new element; quantitative analyses become possible on a wider range of spectral intensities (min–max of intensity between the spectra within the same IR image), typically what we observe on biological samples, where the scale of concentration of organic matter can be from 1 to 5 in absolute value. The MCT detectors are liquid-N_2 cooled for reducing the electronic noise level well below the signal limit of IR sources (Globar, synchrotron radiation and tunable lasers) [33]. It is therefore a technology of choice for fast acquisitions (short scanning duration with low level of accumulated signal) or to analyze very thin samples (with small amount of IR-active vibrators to create a detectable signal). Microbolometer detectors have a noise floor much higher than MCT. Therefore, they have not been considered useful for FTIR microscopes using globar sources since high S/N could not be obtained. Now that the signal level of QCL sources is several orders of magnitude higher, the use of uncooled FPA microbolometer detectors can be considered. Now the noise and signal stability issues are solved while coupling QCLs with a microbolometer-FPA, the main advantage is that uncooling the detector allows long-duration acquisitions in much more stable conditions. The speed and minimal down-time advantage of the QCL-IR microscope using the microbolometer camera allows for the analysis of larger samples. However, the QCL sources remain limited compared to FTIR spectrometers. The wavelength coverage is currently about 1800–900 cm^{-1} through a combination of 4 QCLs while an FTIR spectrometer can cover 500–8000 cm^{-1}. QCLs are also limited in spectral resolution to 4 cm^{-1} in the first generation of commercially available microscopes while FTIR microscopes offer a 1-cm^{-1} resolution. Nevertheless, the analysis of tissues is not requiring a high spectral resolution and most of chemical bonds found in molecules exhibit IR bands in the fingerprint region, the 1800–900 cm^{-1} spectral interval now covered by QCLs. Histopathology being considered as a main avenue for routine applications of IR microscopy, thus possibly bringing dedicated analytical setups in clinics, such quantitative analysis could very well define a key domain of the development of the IR microscopy emanating from all the efforts that the academic research devoted over the past 10–15 years.

Is there a specific coherent-like source *vs.* dispersive source effects on spectral baseline? We have observed differences in spectra obtained by FTIR and QCL-powered microscopes. These differences show that the signal intensity is not registered equivalently when collecting signal wavelength-by-wavelength of from an interferogram and a Fourier-transform. Quantum cascade lasers are spatially coherent sources, unlike the thermal Globar sources, which are dispersive. This is thus affecting the way IR photons interact with the sample contents. The main question is about how to comprehend this difference: it is an improvement or not, or is it just different because of the source type? To try to provide an answer, it is first important to remind what is making the signal and what is making the noise in a spectrum obtained in transmission

measurement. In principle, QCLs should have the advantage of the sensitivity (and thus the S/N) because of the high photon flux they provide compared to Globar sources [34]. But, we normalized the S/N in our comparison, even if a large number of scans was required with the FTIR system. Another reason can be the baseline fluctuation, which is not only due to the noise of the system, but also the sample and thus the way IR photons interact with it. As shown in Fig. 1, the focus of the beam on the sample is not similar between systems, a larger angle of focusing being used with the FTIR. However, it is not clear for the moment what can be the effect on tissue analysis, which has the advantage to be rather flat (thus limiting border effects that induce photon diffraction, which could alter the signal measurement on detector). Nevertheless, changes in optical density and index can appear in tissue sections, even at thin thickness (histology uses thicknesses ranging between 4 and 20 μm). This is due to the presence of different objects in the tissue at dimensions close to the diffraction limit of the wavelengths corresponding to the mid-IR region (5.5–11 μm), sucg as cell nucleus (Ø 1–4 μm), mitochondria (Ø 1–3 μm), blood vessels (Ø 5–20 μm)…etc. A dispersive IR source might generate a random diffraction of IR photons at the contact of these objects while the coherent QCL source should have a more narrow pattern of diffraction. But this remain to be confirmed on experimental objects (ex. beads of different size and density in gels for example). As observed on the curve-fitting results, this is also modifying the shape of IR bands, although it did not affected significantly the overall results of these data treatments between IR microscopy systems. It means that all previous data treatment methods have to be recalibrated or adapted to the new structure of spectral data obtained while using laser sources.

3.2. *Fast QCL-IR microscopy: the route to 3D histology?*

The main avenue for large scale application seems to be histopathology in clinics, with the objective to perform automated or semi-automated diagnostics on biopsies. The development of the first quantitative histology method can be achieved by extracting the chemical parameters found in IR spectra and determining their distribution. One simple example of this unique feature is that quantitative metabolic analyses can be performed, which no current histological technique can do. It will also allow foreseeing the development of 3D reconstruction methods, where stacking 2D images for a 3D overview of the sample contents can make the breakthrough towards 3D pathology. Histological 3D datasets can be formed by collection of individual 2D slice images, and chemical parameters can be reconstructed for determining solid substructures in tissues, such as blood or lymph vessels, membranes or connective tissues, cells [4]…etc. as previously demonstrated [35]. In that sense, IR microscopy might challenge currently existing histological methods for revealing tissue contents by coloration or labels, but without using these ones, and also adding quantitative chemical parameters assigned to metabolic, biochemical or molecular features of the tissue. This will require a lot of methods to be developed and validated, from spectral information extraction to 3D reconstruction and visualization. These developments will also require developing an appropriate technological environment, with automation of data acquisitions and storage, as well as with high-throughput calculation center allowing to handle the bigdata files generated by 3D IR images (Fig. 5). Automation, high-throughput, and bigdata will become the three pillars of the development of 3D IR imaging for anatomo-pathology in clinics. Furthermore, must faster QCLs are announced, reducing the scanning time per wavelength to a few ms only without S/N alteration. This would reduce again the acquisition time and thus bring this technology closer to hospitals for routine anatomo-pathology.

4. Conclusion

The new generation of IR microscopes promises faster acquisitions that open the potential of this technique to new applications and developments. By reducing the acquisition time on large sample areas, reproducible – and thus quantitative – approaches are allowed. This is giving to IR microscopy a unique advantage over other analytical techniques, notably for the ability to determine absolute concentrations of chemical and molecular species in biosamples. However, it also appears that the coherence of laser sources is modifying the shape of the spectral data resulting from sample measurements. This has to be taken into account in future studies using such technology. However, high-speed data acquisitions make conceivable to develop 3D reconstruction methods (stacking 2D IR images from consecutive sample sections) for a 3D chemical imaging with quantitative analyses. Thus, IR imaging will become a credible challenger of the only other quantitative modality available in chemical microscopy, namely mass-spectroscopy

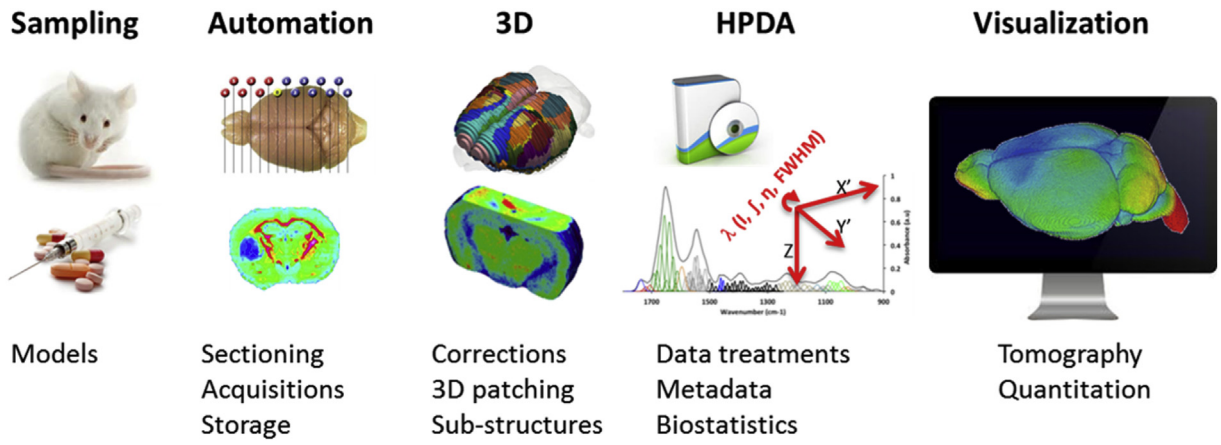

Fig. 5. Proposed technological chain for developing 3D IR anatomo-pathology in clinics. The main issues for implementing IR microscopy as a 3D chemical imaging method are defined by the 5 columns of R&D efforts for providing a 3D IR tomography resource. The sampling methods and use-cases must be developed for 3D histology; automation must be achieved for continuous sectioning, IR image acquisitions and data storage; 3D reconstruction methods will depend mostly on individual image corrections allowing a 3D patching at microscopic resolution for extracting tissue substructures as small as blood capillaries; high-performance data analytics must be invented to allow 3D features analyses from spectral-derived data and metadata; and visualization routines must be developed from spectral data/metadata selection to highlight relevant parameters in 3D [35].

imaging, but with a significant simplification of sample preparation and spectral data treatments.

Acknowledgements

The author is indebted to the contribution of “Ligue Nationale contre le cancer” and the “Agence Nationale de la Recherche” (ANR – contract n°2013-001-3DXIR-Pathology) for their financial supports.

Appendix A. Supplementary data

Supplementary data related to this article can be found at http://dx.doi.org/10.1016/j.trac.2017.02.007.

References

[1] C.C. Chien, H.H. Chen, S.F. Lai, K.C. Wu, X. Cai, Y. Hwu, C. Petibois, Y.S. Chu, G. Margaritondo, Gold nanoparticles as high-resolution X-ray imaging contrast agents for the analysis of tumor-related micro-vasculature, J. Nanobiotechnol. 10 (2012).
[2] D. Taverna, F. Boraldi, G. De Santis, R.M. Caprioli, D. Quaglino, Histology-directed and imaging mass spectrometry: an emerging technology in ectopic calcification, Bone 74 (2015) 83–94.
[3] M. Verdonck, S. Garaud, H. Duvillier, K. Willard-Gallo, E. Goormaghtigh, Label-free phenotyping of peripheral blood lymphocytes by infrared imaging, Analyst 140 (2015) 2247–2256.
[4] H.H. Chen, V. Bobroff, M. Delugin, R. Pineau, R. Noreen, Y. Seydou, S. Banerjee, J. Chatterjee, S. Javerzat, C. Petibois, The future of infrared spectroscopy in biosciences: in vitro, time-resolved, and 3D, Acta Phys. Pol. A 129 (2) (2016) 255–259.
[5] V. Bobroff, C. Rubio, V. Vigier, C. Petibois, FTIR Spectroscopy characterization of fatty-acyl-chain conjugates, Anal. Bioanal. Chem. 407 (2016) 1–6.
[6] C. Petibois, M. Cestelli Guidi, Bioimaging of cells and tissues using accelerator-based sources, Anal. Bioanal. Chem. 391 (2008) 1599–1608.
[7] R. Bhargava, Towards a practical Fourier transform infrared chemical imaging protocol for cancer histopathology, Anal. Bioanal. Chem. 389 (2007) 1155–1169.
[8] T.D. Wang, G. Triadafilopoulos, J.M. Crawford, L.R. Dixon, T. Bhandari, P. Sahbaie, S. Friedland, R. Soetikno, C.H. Contag, Detection of endogenous biomolecules in Barrett's esophagus by Fourier transform infrared spectroscopy, Proc. Natl. Acad. Sci. U. S. A. 104 (2007) 15864–15869.
[9] B.R. Wood, L. Chiriboga, H. Yee, M.A. Quinn, D. McNaughton, M. Diem, Fourier transform infrared (FTIR) spectral mapping of the cervical transformation zone, and dysplastic squamous epithelium, Gynecol. Oncol. 93 (2004) 59–68.
[10] C.P. Schultz, K.Z. Liu, E.A. Salamon, K.T. Riese, H.H. Mantsch, Application of FT–IR microspectroscopy in diagnosing thyroid neoplasms, J. Mol. Struct. 480–481 (1999).
[11] E.P. Paschalis, O. Jacenko, B. Olsen, R. Mendelsohn, A.L. Boskey, Fourier transform infrared microspectroscopic analysis identifies alterations in mineral properties in bones from mice transgenic for type X collagen, Bone 19 (1996) 151–156.
[12] E. David-Vaudey, A. Burghardt, K. Keshari, A. Brouchet, M. Ries, S. Majumdar, Fourier Transform Infrared Imaging of focal lesions in human osteoarthritic cartilage, Eur. Cells Mater. 10 (2005) 51–60. Discussion 60.
[13] K.M. Gough, D. Zelinski, R. Wiens, M. Rak, I.M. Dixon, Fourier transform infrared evaluation of microscopic scarring in the cardiomyopathic heart: effect of chronic AT1 suppression, Anal. Biochem. 316 (2003) 232–242.
[14] C.R. Flach, D.J. Moore, Infrared and Raman imaging spectroscopy of ex vivo skin, Int. J. Cosmet. Sci. 35 (2013) 125–135.
[15] K.Z. Liu, A. Man, A. Shaw, B. Liang, Z. Xu, Y. Gong, Molecular determination of liver fibrosis by synchrotron infrared microspectroscopy, Biochim. Biophys. Acta 1758 (2006) 960–967.
[16] J. Kneipp, L.M. Miller, M. Joncic, M. Kittel, P. Lasch, M. Beekes, D. Naumann, In situ identification of protein structural changes in prion-infected tissue, Biochim. Biophys. Acta 1639 (2003) 152–158.
[17] C. Petibois, B. Desbat, Clinical application of FTIR imaging: new reasons for hope, Trends Biotechnol. 28 (2010) 495–500.
[18] C. Petibois, Imaging methods for elemental, chemical, molecular, and morphological analyses of single cells, Anal. Bioanal. Chem. 397 (2010) 2051–2065.
[19] B. Drogat, M. Bouchecareilh, C. Petibois, G. Déléris, E. Chevet, A. Bikfalvi, M. Moenner, Acute L-glutamine deprivation compromises VEGF-a up-regulation in A549/8 human carcinoma cells, J. Cell Physiol. 212 (2007) 463–472.
[20] D.C. Malins, N.L. Polissar, S. Schaefer, Y. Su, M. Vinson, A unified theory of carcinogenesis based on order-disorder transitions in DNA structure as studied in the human ovary and breast, Proc. Natl. Acad. Sci. U. S. A. 95 (1998) 7637–7642.
[21] C. Petibois, G. Déléris, Chemical mapping of tumor progression by FT-IR imaging: towards molecular histopathology, Trends Biotechnol. 24 (2006) 455–462.
[22] A.L. Boskey, S. Gadaleta, C. Gundberg, S.B. Doty, P. Ducy, G. Karsenty, Fourier transform infrared microspectroscopic analysis of bones of osteocalcin-deficient mice provides insight into the function of osteocalcin, Bone 23 (1998) 187–196.
[23] A. Derenne, O. Vandersleyen, E. Goormaghtigh, Lipid quantification method using FTIR spectroscopy applied on cancer cell extracts, Biochim. Biophys. Acta 1841 (2014) 1200–1209.
[24] N. Wald, E. Goormaghtigh, Infrared imaging of primary melanomas reveals hints of regional and distant metastases, Analyst 140 (2015) 2144–2155.
[25] M. Cestelli Guidi, S. Yao, D. Sali, S. Castano, A. Marcelli, C. Petibois, Experimental ATR device for real-time SR-FTIR imaging of living cells, Biotechnol. Adv. 31 (2013) 402–407.
[26] C. Petibois, G. Deleris, M. Piccinini, M. Cestelli Guidi, A. Marcelli, A bright future for synchrotron imaging, Nat. Photonics 3 (2009) 179.
[27] B. Bird, M.J. Baker, Quantum cascade lasers in biomedical infrared imaging, Trends Biotechnol. 33 (2015) 557–558.
[28] Y. Yao, A.J. Hoffman, C.F. Gmachl, Mid-infrared quantum cascade lasers, Nat. Photonics 6 (2012) 432–439.
[29] M.R. Kole, R.K. Reddy, M.V. Schulmerich, M.K. Gelber, R. Bhargava, Discrete frequency infrared microspectroscopy and imaging with a tunable quantum cascade laser, Anal. Chem. 84 (2012) 10366–10372.
[30] D.T.D. Childs, R.A. Hogg, D.G. Revin, I. Ur Rehman, J.W. Cockburn, S.J. Matcher, Sensitivity advantage of QCL tunable-laser mid-infrared spectroscopy over FTIR spectroscopy, Appl. Spectrosc. Rev. 50 (2015) 822–839.
[31] N. Kroger, A. Egl, M. Engel, N. Gretz, K. Haase, I. Herpich, B. Kranzlin, S. Neudecker, A. Pucci, A. Schonhals, J. Vogt, W. Petrich, Quantum cascade laser-based hyperspectral imaging of biological tissue, J. Biomed. Opt. 19 (2014) 111607.
[32] C. Petibois, M. Cestelli Guidi, M. Piccinini, M. Moenner, A. Marcelli, Synchrotron radiation FTIR imaging in minutes: a first step towards real-time cell imaging, Anal. Bioanal. Chem. 397 (2010) 2123–2129.
[33] A. Marcelli, A. Cricenti, W.M. Kwiatek, C. Petibois, Biological applications of synchrotron radiation infrared spectromicroscopy, Biotechnol. Adv. 30 (2013) 1390–1404.
[34] A. Schwaighofer, M.R. Alcaraz, C. Araman, H. Goicoechea, B. Lendl, External cavity-quantum cascade laser infrared spectroscopy for secondary structure analysis of proteins at low concentrations, Sci. Rep. 6 (2016) 33556.
[35] V. Bobroff, H.H. Chen, M. Delugin, R. Pineau, S. Javerzat, C. Petibois, 3D digital histology by quantitative IR microscopy and spectromics, J. Biophotonics (2016) 1–9.